SOME RESEARCH ON TWO-DIMENSIONAL LAMINAR SEPARATION BUBBLES

by

E. Dobbinga
J.L. van Ingen
J.W. Kooi

AGARD Conference Proceedings CP102
Lisbon 1972

Note: The research on airfoils at low Reynolds numbers as occur for sailplanes revealed the importance of laminar separation bubbles. The paper reprinted next describes an empirical correlation with Reynolds number of the angle at which a laminar separation streamline leaves the wall. This research has laid the foundation for incorporating separation bubbles in airfoil design, including the phenomenon of bursting.

SOME RESEARCH ON TWO DIMENSIONAL LAMINAR SEPARATION BUBBLES

E. Dobbinga, J.L. van Ingen and J.W. Kooi
Department of Aeronautical Engineering, Technological University of Delft, Kluyverweg 1, Delft, The Netherlands.

SUMMARY

For the development of a calculation method for the laminar part of separation bubbles in two-dimensional incompressible flow, it was found necessary to gather empirical information on the angle γ at which the separation streamline leaves the wall.

On seven different models in three different low speed windtunnels the angle γ has been determined from smoke photographs taken with a camera which was specially built for this purpose. The flows which were investigated are:

(a) plane stagnation point boundary layer flow; separation induced by means of a forward facing step.
(b) a cylinder (diameter 70 mm) with a tail; "natural" separation on the cylindrical nose part.
(c) a cylinder (diameter 400 mm) with a tail; "natural" separation on the cylindrical nose part.
(d) a long cylinder with rounded nose, aligned axially with the wind; separation induced by a forward facing step.
(e) a short flat plate, separation induced by means of auxiliary airfoils.
(f) the same flat plate as in (e); separation induced by a forward facing step.
(g) a long flat plate; separation induced by a forward facing step.

The measured angles γ are plotted as a function of the Reynolds number $\frac{U\theta}{\nu}$ at separation $= (R_\theta)_{sep}$. The investigations cover a range of $(R_\theta)_{sep}$ from 35 up to about 700. All measured points fall reasonably well on a single curve.

NOTATION

B	constant in Eq. (3)
c	reference length, radius of cylinder for confs. (b) and (c)
h	step height
p	static pressure
R_θ	$\frac{U\theta}{\nu}$
R_c	$\frac{U_\infty c}{\nu}$
u	velocity component parallel to wall in boundary layer
U	velocity component parallel to wall at edge of boundary layer
U_∞	reference speed
$\bar{u}$	$\frac{u}{U}$
$\bar{U}$	$\frac{U}{U_\infty}$
x	distance along the wall
y	distance normal to the wall
γ	angle at which the separation streamline leaves the wall (defined in Fig. 5)
θ	$\int_0^\infty \bar{u}(1-\bar{u})\,dy$, momentum loss thickness
ν	coefficient of kinematic viscosity
τ_o	wall shear stress

Subscript sep denotes conditions at the separation point.

1. INTRODUCTION

It is not necessary to stress in this paper the importance of the laminar separation bubble for the subject of aircraft stalling. It is well known that an overriding influence on the stalling behaviour is excerted by the type of flow in the separation bubble, that is to say whether or not the separated flow will reattach to the surface after it has become turbulent. Our own interest in the subject is related to the development of a computer program for the design of airfoil sections (Ref. 1,2). We can distinguish three main topics in the investigation of separation bubbles. (Fig. 1)

1) the laminar flow leaving the wall,
2) transition to turbulent flow in the separated shear layer,
3) reattachment or failure to reattach of the turbulent flow.

Topic 3 is discussed by Horton in Ref. 3 where a method is described which enables us to determine whether turbulent reattachment will occur. To apply this method, the position of transition in the separated flow has to be known.

Our own research is mainly concerned with topics 1 and 2. The second topic will be the subject of an investigation which will be started later this year. It is intended to try and extend the second author's transition prediction method for attached flows (Ref. 4,5) to the case of separated flows. In this method the amplification of unstable disturbances in the laminar flow, as calculated by means of linear stability theory, is used to predict transition. A similar method has been developed independently by Smith and Gamberoni (Ref. 6).

The present paper deals with the first topic: the investigation of the separated laminar flow field.

2. SOME THEORETICAL CONSIDERATIONS

Calculating the separation point by means of laminar boundary layer theory has been the subject of many investigations; a review of this work may be found in the article by Brown and Stewartson (Ref. 7). When the pressure distribution is prescribed, generally a singularity will occur at separation such that the wall shear stress τ_o tends to zero like

$$\tau_o \sim (x_{sep} - x)^{\frac{1}{2}} \tag{1}$$

This was shown first by Goldstein (Ref. 8); Eq. (1) is confirmed by accurate numerical solutions of the boundary layer equations, such as given by Leigh (Ref. 9) and Terrill (Ref. 10). With these numerical methods it was impossible to calculate through the separation point; in fact the step size for the calculation in x-direction had to be reduced to very small values when approaching the separation point. It seems that the question has not yet been answered whether the boundary layer equations can describe a separating flow if the true (measured) pressure distribution is used. One might find however that already small deviations from the true pressure distribution would cause the difficulties to arise again. Moreover, it is difficult to determine a priori the pressure distribution which will occur.

Some light is thrown on the real behaviour of the flow in the neighbourhood of the separation point by the work of Legendre (Ref. 11) and Oswatitsch (Ref. 12). By using a Taylor series expansion for the solution of the Navier-Stokes equations around the separation point, they proved that the separation streamline leaves the wall at an angle γ which is given by

$$\tan(\gamma) = -3 \frac{\frac{d\tau_o}{dx}}{\frac{\partial p}{\partial x}} \tag{2}$$

The right-hand side of Eq. (2) has to be evaluated at the separation point. In this equation τ_o denotes the wall shear stress; x is the distance along the wall and p is the static pressure which (because Eq. (2) is based on the full Navier-Stokes equations) may be a function of x and y.

According to Eq. (1) accurate boundary layer calculation methods, when not applied to the actual pressure distribution, tend to lead to $\frac{d\tau_o}{dx} \to -\infty$ at separation so that Eq. (2) would predict a separation angle γ of 90°; this is in contradiction with experimental evidence. Therefore, if we want to calculate the separated flow, we have to use one of the following approaches.

1. Investigate whether boundary layer calculations based on the actual pressure distribution lead to a useful result; this would still leave us with the difficulty of providing this pressure distribution.
2. Use the full Navier-Stokes equations in the neighbourhood of the separation point and match the result to those of boundary layer calculations farther away.
3. Use some empirical information of a sufficiently general nature so that simple calculation methods might be used for the separated flow.

The third approach was followed in our work. The simple calculation method, which will be outlined in section 4, employs an empirical relation between the separation angle γ and some parameter which can be found from a boundary layer calculation upstream of the separation point. It seems appropriate to choose for this parameter the Reynolds number $\frac{U\theta}{\nu}$ at separation, denoted by $(R_\theta)_{sep}$. This parameter will not be influenced too much by details of the flow in the direct vicinity of the separation point. Therefore it can be expected that a boundary layer calculation, based on a prescribed pressure distribution, will give $(R_\theta)_{sep}$ with sufficient accuracy.

To get an idea about the type of relation to be expected between $(R_\theta)_{sep}$ and γ we will make the following (questionable !) assumptions.

(1) Boundary layer theory remains valid at separation.
(2) The non-dimensional pressure distribution around a given body at a given angle of attack is independent of the Reynolds number R_c.

These assumptions lead to the following relation

$$\tan(\gamma) = \frac{B}{(\frac{U\theta}{\nu})_{sep}} \tag{3}$$

in which B is a constant for a given body at a given angle of attack. In view of assumption (2) it follows that the "constant" B in Eq. (3) may be different for separation bubbles developing on different bodies or on the same body at different angles of attack.

It may be argued that B should be the same for all bubbles, developing under different nondimensional pressure distributions, if the following additional assumptions (3) and (4) are made.

(3) The flow can be described by a one-parameter boundary layer calculation method such as Pohlhausen's.
(4) The graph of the velocity U at the edge of the boundary layer as a function of x has a point of inflexion at separation. (Some evidence in favour of assumption (4) seems to follow from our experiments).

Although the assumptions (1) through (4) may be questionable, it was thought that Eq. (3) might be a good reference frame in which to place our experimental results.

3. THE EXPERIMENTAL APPARATUS AND SOME RESULTS

Measurements have been performed on seven different model configurations (a) through (g) in three different low speed windtunnels. These configurations have been indicated schematically in Fig. 2. Some details about the models and experimental techniques have been collected in Table 1. In all cases considered, the shape of the front part of the laminar separation bubble has been determined photographically. From the photographs the angle γ between the dividing streamline and the wall at the separation point could be determined. Examples of flow pictures for configurations (b) and (d) are shown in Fig. 4. The angle γ is defined in Fig. 5.

The flow has been made visible by means of tobacco smoke introduced into the separation bubble. A narrow region around the plane of measurement has been illuminated by means of a small electronic flash with 1/900 sec flash duration.
In situation (a) the flash was installed inside the model and the light passed through two diafragms with narrow slits (0.3 mm wide) and through the transparent (perspex) front plate of the model.
In the situations (b) through (g) the flash-with-diafragm was installed outside the tunnel; in these cases long-focus lenses have been used to focus the light in the front part of the separation bubble in a narrow region around the plane of measurement.
Flow pictures have been taken with rather long camera's especially built for the purpose; in fact in all cases the pictures on the film were larger than the original flow phenomena so that rather fine flow details can be distinguished. A schematic drawing of the photographic equipment as used with configuration (g) is shown in Fig. 3.

The main results of the present investigation are shown in Fig. 6 where measured values of $\tan(\gamma)$ are plotted vs. the corresponding value of the Reynolds number at separation $(R_\theta)_{sep}$. In all cases a rather large number of photographs was taken for each flow situation.
With respect to the upper end of the range of $(R_\theta)_{sep}$ it should be noted that at high Reynolds numbers the boundary layer will become turbulent so that no laminar separation will occur. Along a flat plate in a stream of low turbulence, transition will occur for $\frac{U\theta}{\nu}$ between 1100 and 1300. With an adverse pressure gradient transition will occur earlier; hence $(R_\theta)_{sep} = 1100$ is an upper limit for a plot like that of Fig. 6. In that figure no points for $(R_\theta)_{sep} > 720$ have been given because in that region the introduction of a sufficient amount of smoke without disturbing the flow gave severe problems. Moreover the angle γ in that region is so small that good accuracy of the measurements can hardly be expected.
For most of the configurations tested the Reynolds number has been varied by changing the wind speed. In configuration (d) also the length x over which the boundary layer developed could easily be changed. In fact measurements have been made at x = 150 mm; 550 mm and 950 mm. However, only the results for x = 150 mm have been given in Fig. 6. The results for configuration (d) at x = 550 and 950 mm, which were included in the pre-print of the paper, have been left out now. Already in the pre-print some doubt had been expressed with regard to the validity of these results: "the flow at separation was not very steady and not very two-dimensional around the circumference of the central body". Since then additional detailed measurements have shown that one should read here: "at large values of x for configuration (d) the flow at separation was not two-dimensional at all".
With respect to the steps used in the experiments, the following remarks can be made. In order to obtain a situation which sufficiently resembles "natural" separation, the step height h should not be too small; h should be such that the step generates an adverse pressure field which extends over a distance normal to the wall which is larger than the boundary layer thickness. If the step height is chosen too small the angle γ is found to increase. Several series of measurements with different step heights in the configurations (d), (f) and (g) showed that in these cases it was certainly sufficient to make h equal to three times the boundary layer thickness at separation.
The results shown in Fig. 6 for the configurations (d), (f) and (g) all refer to situations in which the steps were sufficiently high. For configuration (a) the influence of h has not been measured; the step height used in that case was 4 mm, which, at all speeds was more than the boundary layer thickness at separation. However, in the light of the observations given above h may have been a little too small at the lowest wind speed. If this is true, the points given in Fig. 6 for the lowest values of $(R_\theta)_{sep}$ might be somewhat too low.

In general, it can be seen from Fig. 6 that the measurements indicate a reasonably unique relation between γ and $(R_\theta)_{sep}$. The value of the "constant" B in Eq. (3) is about 15 to 20.

Some results of pressure distribution measurements on configuration (c) are shown in Fig. 7 in the form of dimensionless velocity $\bar{U}$ at the edge of the boundary layer. The values of $\bar{U}$ have been determined from the measured pressure distribution along the wall by assuming that p is constant across the boundary layer and applying Bernoulli's theorem outside the boundary layer. The measured distributions show a characteristic flattening especially when the Reynolds number is low. This flattening is reproduced by the calculation method to be described in section 4.

4. APPROXIMATE CALCULATION OF THE LAMINAR FLOWFIELD DOWNSTREAM OF SEPARATION

A calculation method has been developed which can approximately predict the laminar flowfield downstream of separation. This method employs the von Kármán momentum integral relation and the first "compatibility condition" of the boundary layer equations. This condition relates the curvature of the velocity profile at the wall to the streamwise pressure gradient. The following additional assumptions are made.

1. The angle γ can be determined from $(R_\theta)_{sep}$ by an empirical relation such as Eq. 3.
2. The "separation streamline" as defined in Fig. 5 remains straight over the full length of the laminar part of the bubble.
3. The reverse flow velocity profiles can be represented by the Stewartson second branch solutions of the Falkner-Skan equation.

In view of our experimental results assumption 2 seems to be reasonable. It would not be difficult however to extend the method to curved separation streamlines.

It should be observed that the pressure distribution in the separated region is not given a priori but it follows from the calculations. In other words: the pressure distribution is determined such that the assumed shape of the separation streamline (for instance straight) is compatible with assumption 1 and 3 and with the equations used.

Initial conditions which are required to start the calculation at the separation point are θ and U. These conditions follow from the boundary layer calculation upstream of the separation point.

Details of the calculation method will not be given here but will be published in a later paper by the second author.

Some preliminary results of the method are shown in Fig. 7 where the calculated pressure distribution is compared to results of some measurements on configuration (c).

5. REFERENCES

1. Ingen, J.L. van: Advanced Computer Technology in Aerodynamics: a program for airfoil section design utilizing computer graphics. VKI Lecture series 16, April 21-25, 1969.
2. Ingen, J.L. van: On the design of airfoil sections utilizing computer graphics. De Ingenieur, vol. 81, nr. 43, 24 october 1969, p. L 110-L 118.
3. Horton, H.P.: A semi-empirical theory for the growth and bursting of laminar separation bubbles. A.R.C.-CP 1073, 1967.
4. Ingen, J.L. van: A suggested semi-empirical method for the calculation of the boundary layer transition region. Report VTH-74, Dept. of Aeron. Eng., University of Technology Delft, 1956.
5. Ingen, J.L. van: Theoretical and experimental investigations of incompressible laminar boundary layers with and without suction. Report VTH-124, Dept. of Aeron. Eng., University of Technology Delft, 1965.
6. Smith, A.M.O. and Gamberoni, N.: Transition, pressure gradient and stability theory. Report ES 26388, Douglas Aircraft Co., 1956.
7. Brown, S.N. and Stewartson, K.: Laminar separation.In: Annual Review of Fluid Mechanics, vol. 1, Palo Alto, Annual Reviews Inc., 1969, p. 45-72.
8. Goldstein, S.: On laminar boundary layer flow near a position of separation. Quart. J. Mech. Appl. Math., vol. 1, 1948, p. 43-69.
9. Leigh, D.C.: The laminar boundary layer equation: A method of solution by means of an automatic computer. Proc. Camb. Phil. Soc., 51, 1955, p. 320-332.
10. Terrill, R.M.: Laminar boundary layer flow near separation with and without suction. Phil. Trans. A 253, 1960, p. 55-100.
11. Legendre, R.: Décollement laminaire régulier. Comptes Rendus 241, 1955, p. 732-734.
12. Oswatitsch, K.: Die Ablösungsbedingung von Grenzschichten. In: Grenzschichtforschung/Boundary layer research. IUTAM Symposium, Freiburg / Br. 1957, Springer Verlag 1958, p. 357-367.

ACKNOWLEDGEMENT

The authors wish to thank the technical staff of the low speed aerodynamics laboratory for their able assistance during the preparation and execution of the experimental stages of the work described in the present paper. Especially Mr. Peter Strookman should be mentioned in this respect.

configuration	separation induced by	pressure distribution obtained from	θ obtained from
(a) plane stagnation point flow on flat nosed airfoil. 400 x 400 mm tunnel.	forward facing step	orifices in flat nose	calculation by means of Thwaites-type method using the measured pressure distribution.
(b) 70 mm dia.cylinder with tail (to suppress fluctuating wake). 400 x 400 mm tunnel.	natural separation on cylindrical nose.	orifices in cylindrical nose; detailed pressure distributions obtained by rotating nose part.	
(c) 400 mm dia.cylinder with tail (to suppress fluctuating wake). 1810 x 1250 mm tunnel.			
(d) 106 mm dia.cylinder with rounded nose; aligned axially in a windtunnel with cross section 300 mm ∅; by moving the central pipe in streamwise direction w.r.t. the tunnel and the measuring apparatus, the length x over which the boundary layer had developed before separation could be varied.	forward facing step (flat disk).	orifices in surface of central pipe.	measured velocity profiles. (total head from traversing flattened total head tube; static pressure from orifice).
(e) flat plate 400 x 400 mm tunnel	auxiliary airfoils	orifices in surface of plate.	
(f) flat plate 400 x 400 mm tunnel	forward facing step		
(g) flat plate 1810 x 1250 mm tunnel			

Table 1: Some details about the experimental apparatus (see also Fig. 2).

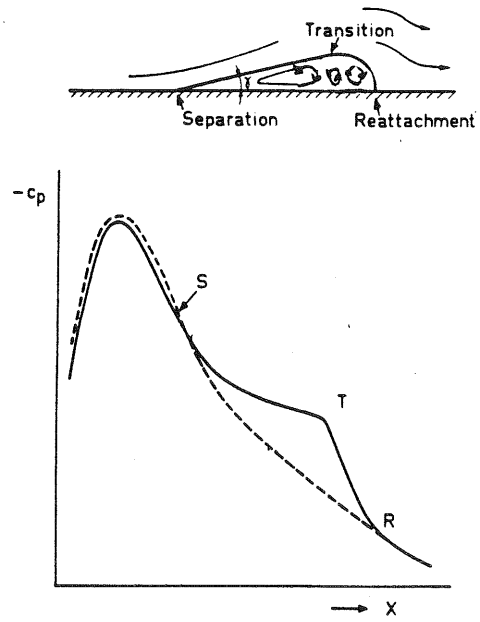

Fig. 1: Schematic diagram of flow field and pressure distribution in a laminar separation bubble.

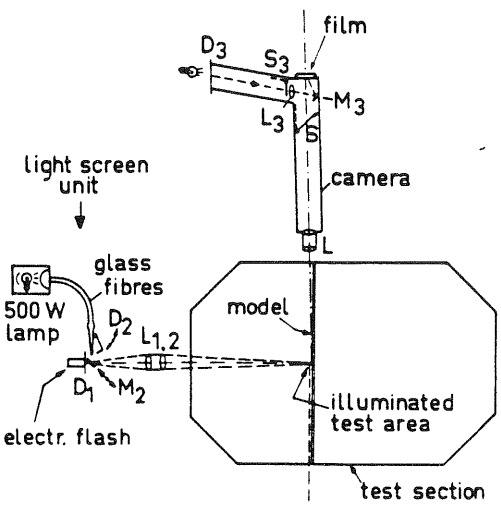

L	lens	1	flash illumination
D	diafragm with narrow slits	2	continuous light
M	mirror	3	projection of reference lines in camera
S	shutter		

Fig. 3: Schematic diagram of photographic equipment used with configuration (g).

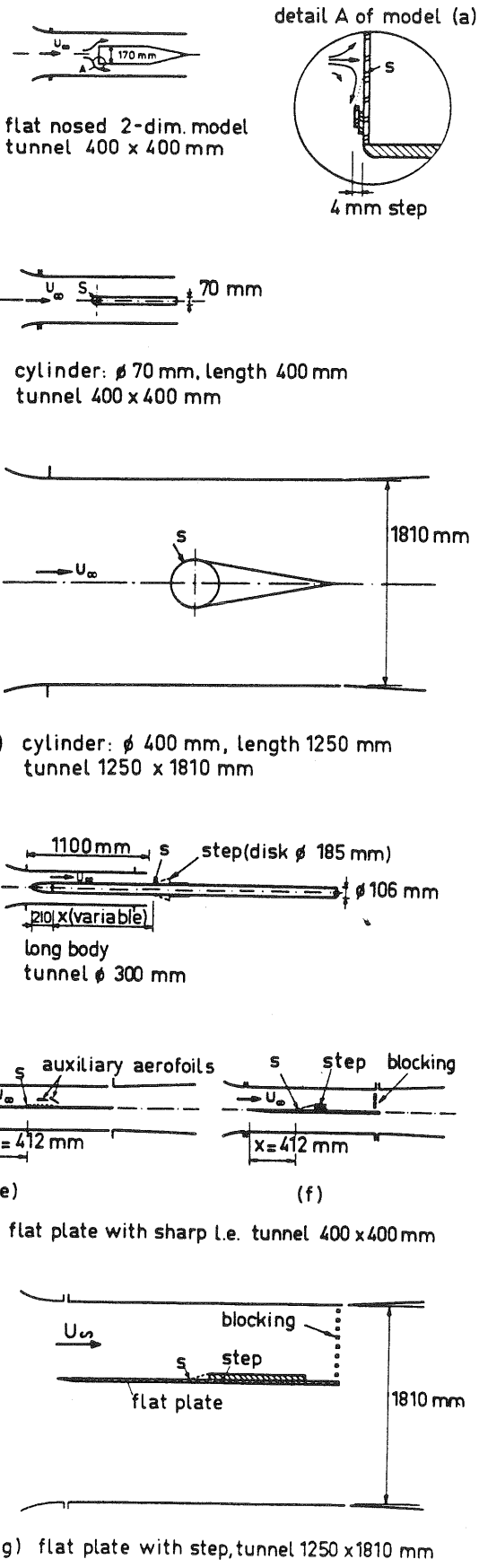

Fig. 2: The experimental configurations.

(plane of measurement in middle of tunnel, S = laminar separation point).

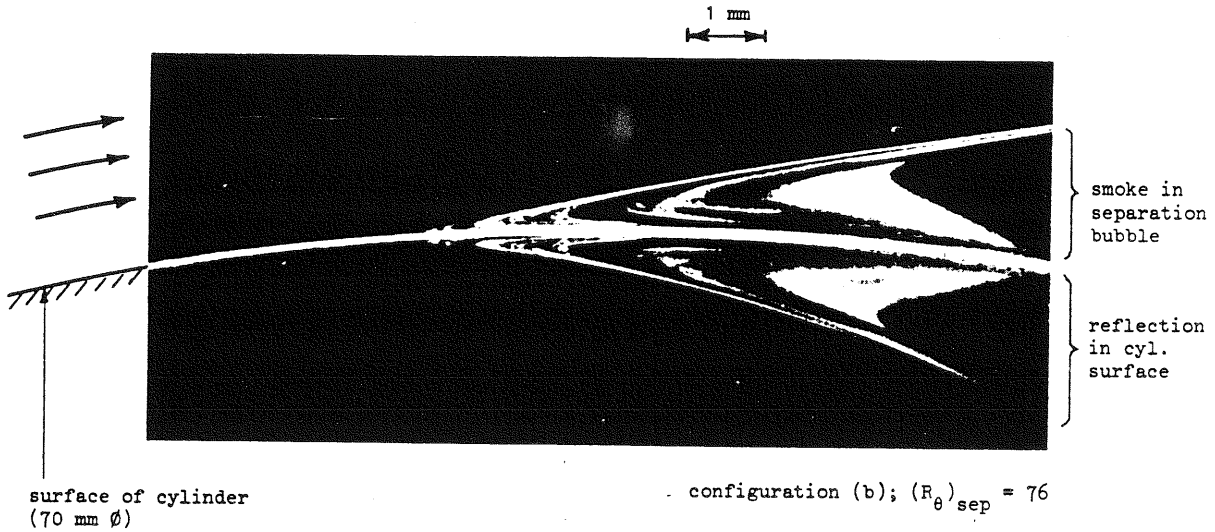

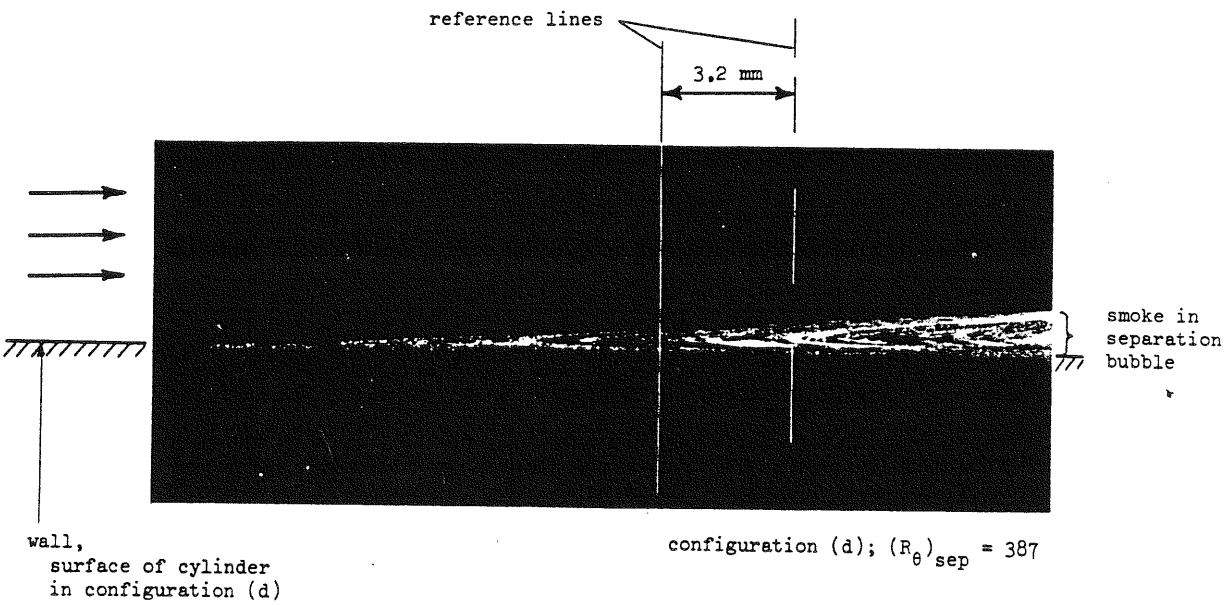

Fig. 4: Examples of flow pictures.

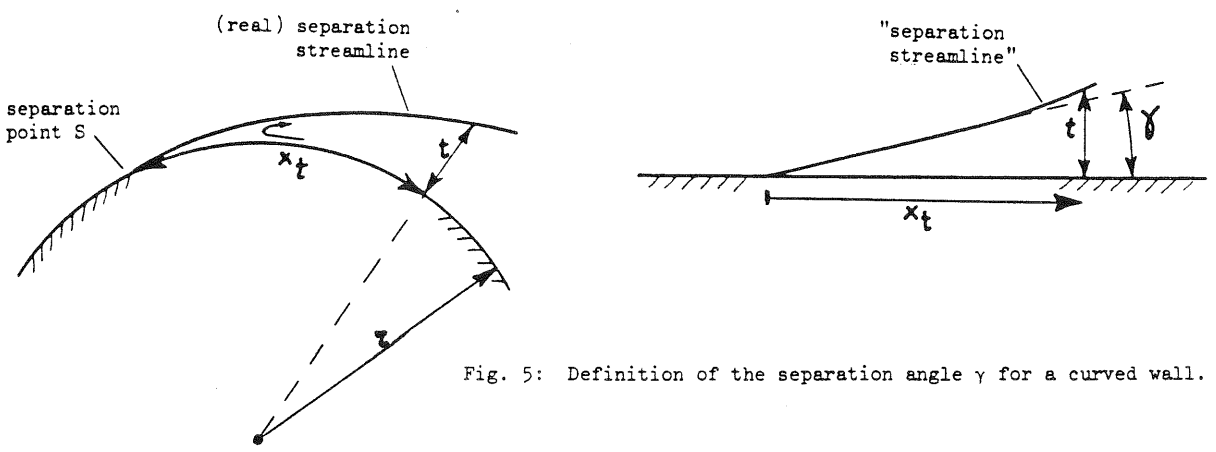

Fig. 5: Definition of the separation angle γ for a curved wall.

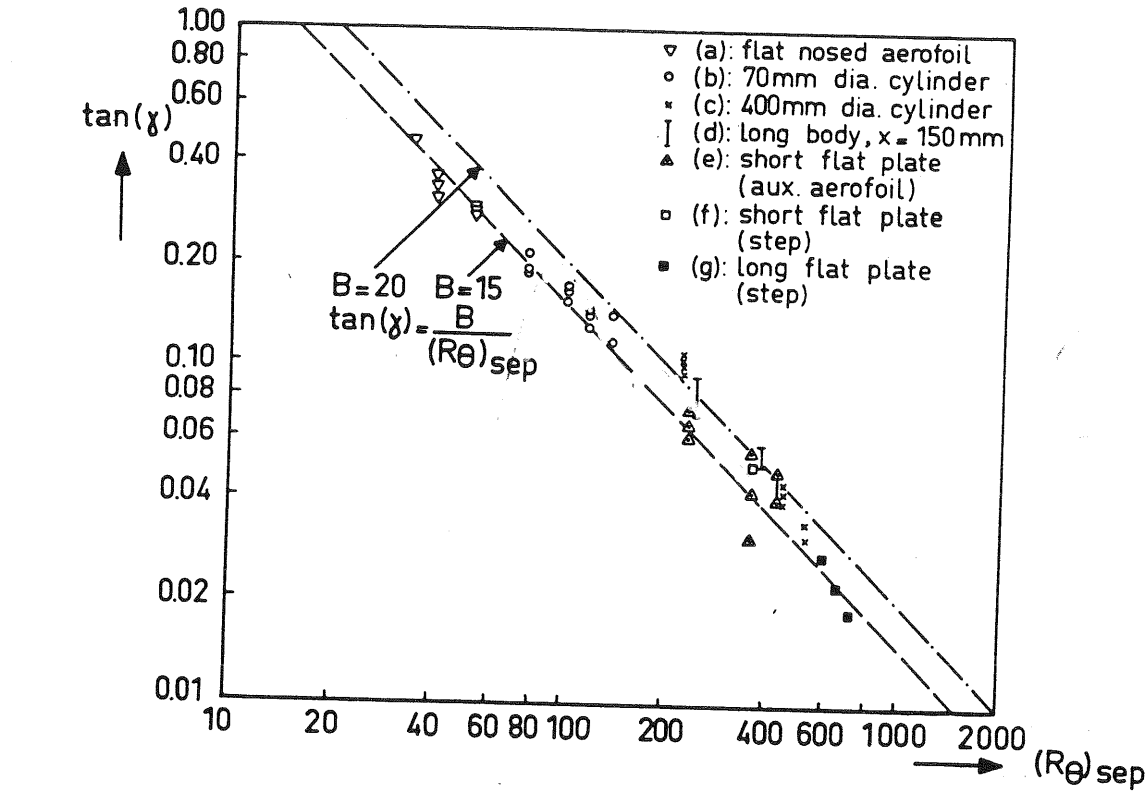

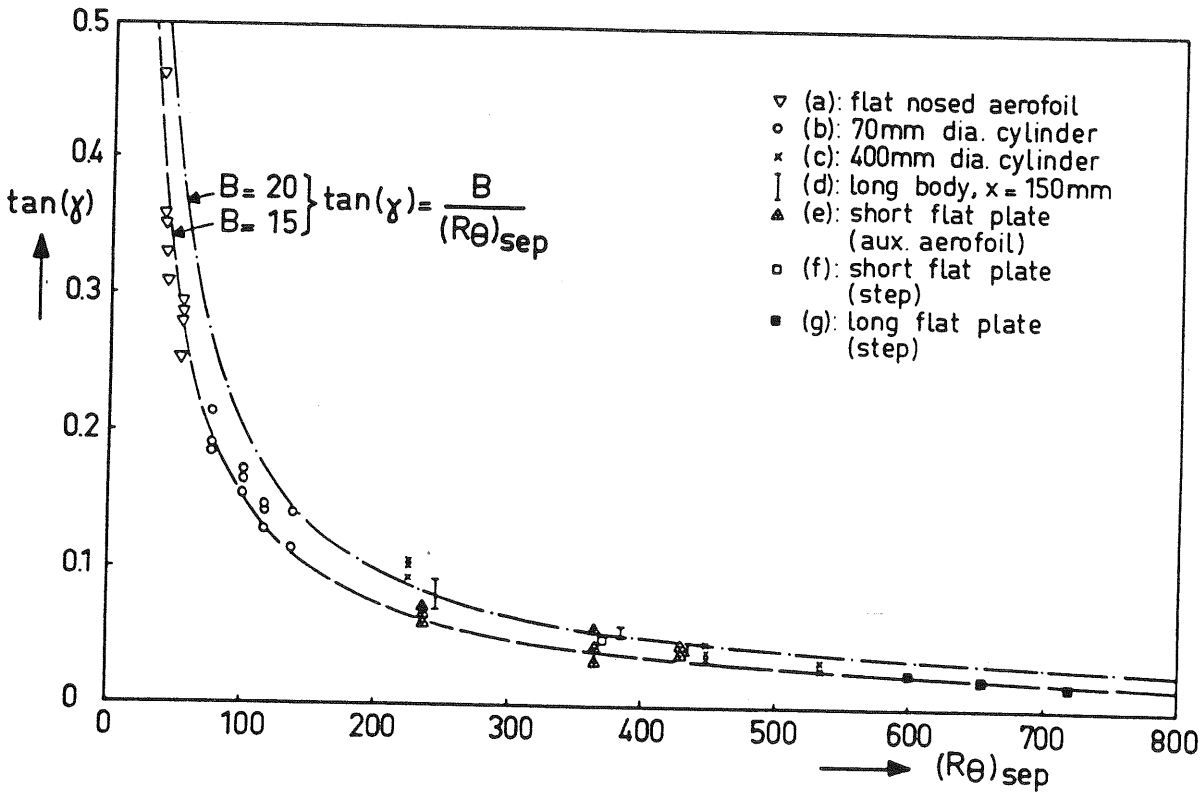

Fig. 6: Separation angle γ as function of the Reynolds number at separation $(R_\theta)_{sep}$.

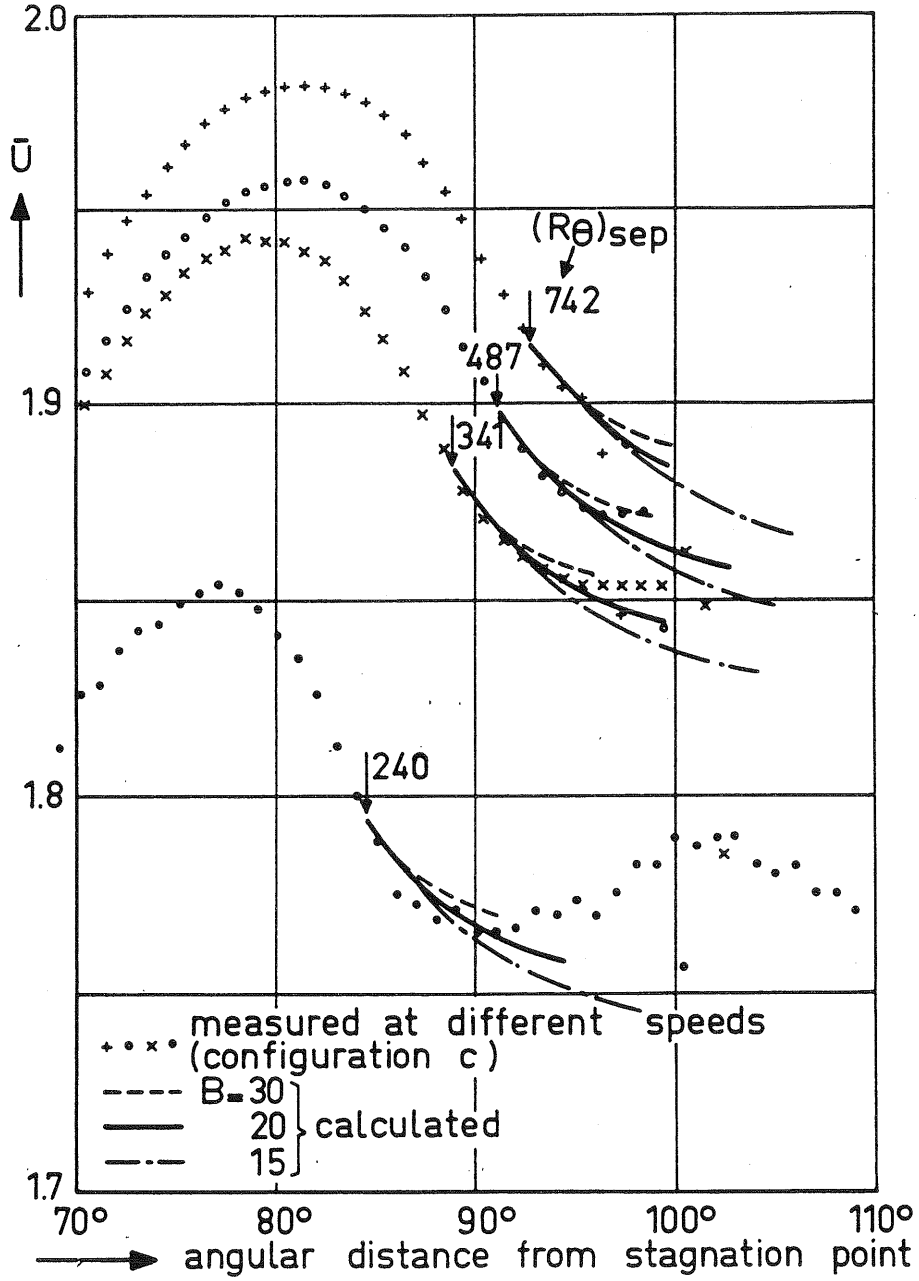

Fig. 7: Some pressure distributions for configuration (c).